


## ORIGINAL ARTICLE

# Hepatic retinoic acid receptor alpha mediates all-trans retinoic acid's effect on diet-induced hepatosteatosis

Fathima N. Cassim Bawa<sup>1,2</sup> | Yanyong Xu<sup>2</sup> | Raja Gopaju<sup>2</sup> |  
 Noel-Marie Plonski<sup>1</sup> | Amy Shiyab<sup>1,2</sup> | Shuwei Hu<sup>2</sup> | Shaoru Chen<sup>2</sup> |  
 Yingdong Zhu<sup>1,2</sup> | Kavita Jadhav<sup>1,2</sup> | Takhar Kasumov<sup>3</sup> | Yanqiao Zhang<sup>2</sup> 

<sup>1</sup>School of Biomedical Sciences, Kent State University Kent, Kent, Ohio, USA

<sup>2</sup>Department of Integrative Medical Sciences, Northeast Ohio Medical University, Rootstown, Ohio, USA

<sup>3</sup>Department of Pharmaceutical Sciences, Northeast Ohio Medical University, Rootstown, Ohio, USA

## Correspondence

Yanqiao Zhang, Department of Integrative Medical Sciences, Northeast Ohio Medical University, 4209 State Route 44, Rootstown, OH 44272, USA.  
 Email: [y Zhang@neomed.edu](mailto:y Zhang@neomed.edu)

## Present address

Yanyong Xu, Key Laboratory of Metabolism and Molecular Medicine of the Ministry of Education, Department of Pathology of School of Basic Medical Sciences, Fudan University, Shanghai, China.

## Funding information

National Institutes of Health, Grant/Award Number: R01DK102619 and R01DK118941

## Abstract

All-trans retinoic acid (AtRA) is an active metabolite of vitamin A that influences many biological processes in development, differentiation, and metabolism. AtRA functions through activation of retinoid acid receptors (RARs). AtRA is shown to ameliorate hepatic steatosis, but the underlying mechanism is not well understood. In this study, we investigated the role of hepatocyte RAR alpha (RAR $\alpha$ ) in mediating the effect of AtRA on hepatosteatosis in mice. Hepatocyte-specific *Rar $\alpha$ <sup>-/-</sup>* (*L-Rar $\alpha$ <sup>-/-</sup>*) mice and their control mice were fed a chow diet, high-fat diet (HFD), or a high-fat/cholesterol/fructose (HFCF) diet. Some of the mice were also treated with AtRA. Loss of hepatocyte RAR $\alpha$ -induced hepatosteatosis in chow-fed aged mice and HFD-fed mice. AtRA prevented and reversed HFCF diet-induced obesity and hepatosteatosis in the control mice but not in *L-Rar $\alpha$ <sup>-/-</sup>* mice. Furthermore, AtRA reduced hepatocyte fatty acid uptake and lipid droplet formation, dependent on hepatocyte RAR $\alpha$ . Our data suggest that hepatocyte RAR $\alpha$  plays an important role in preventing hepatosteatosis and mediates AtRA's effects on diet-induced hepatosteatosis.

## INTRODUCTION

Nonalcoholic fatty liver disease (NAFLD) is the most common chronic liver disease in the world. NAFLD constitutes a spectrum of conditions ranging from non-alcoholic fatty liver or simple steatosis to nonalcoholic steatohepatitis, which may further progress to cirrhosis and hepatocellular carcinoma. So far, the underlying mechanism for the pathogenesis of NAFLD is not fully understood. NAFLD is often associated with insulin resistance and is the hepatic manifestation of metabolic

syndrome. During insulin resistance, hepatic *de novo* lipogenesis and fatty acid uptake are increased to induce hepatosteatosis and lipotoxic lipid accumulation, which may further cause liver inflammation and fibrogenesis.<sup>[1–3]</sup>

Vitamin A is important for many biological processes, such as embryogenesis, cell proliferation and differentiation, vision, immune regulation, and metabolism.<sup>[4]</sup> Patients with NAFLD have often shown disrupted vitamin A homeostasis.<sup>[4–6]</sup> The liver harbors the most vitamin A in hepatic stellate

This is an open access article under the terms of the [Creative Commons Attribution-NonCommercial-NoDerivs](https://creativecommons.org/licenses/by-nc-nd/4.0/) License, which permits use and distribution in any medium, provided the original work is properly cited, the use is non-commercial and no modifications or adaptations are made.

© 2022 The Authors. *Hepatology Communications* published by Wiley Periodicals LLC on behalf of American Association for the Study of Liver Diseases.

cells (HSCs). When HSCs are activated, they lose the retinyl ester stores, leading to fibrosis. Vitamin A exerts its functions through active metabolites—all trans retinoic acid (AtRA) and 9-cis retinoic acid (9-cis-RA), which activate the nuclear hormone receptors retinoic acid receptors (RAR $\alpha$ , RAR $\beta$ , and RAR $\gamma$ ) and retinoid X receptors (RXR $\alpha$ , RXR $\beta$ , and RXR $\gamma$ ), respectively. RARs heterodimerize with RXR and bind to the DNA motifs known as retinoic acid response elements (RAREs) to regulate the expression of genes involved in cell growth or differentiation.

AtRA has been shown to reduce liver steatosis via a pathway involving peroxisome proliferator-activated receptor gamma (PPAR $\gamma$ ) repression in mice,<sup>[7]</sup> and improves liver steatosis in rabbits.<sup>[8]</sup> Treatment of KK-A<sup>y</sup> mice or high-fat/high fructose diet-fed mice with AtRA has been shown to ameliorate insulin resistance.<sup>[9]</sup> Despite these beneficial effects of AtRA, it remains unclear how AtRA improves hepatosteatosis. In addition, the role of genetic loss of hepatocyte RAR $\alpha$  in fatty liver disease has not been investigated. In this study, we investigated the role of loss of hepatocyte RAR $\alpha$  in high-fat/cholesterol/fructose (HFCF) diet-induced hepatosteatosis and in mediating AtRA-induced amelioration of fatty liver disease. Our data show that AtRA treatment prevents and reverses HFCF diet-induced hepatosteatosis via hepatocyte RAR $\alpha$ -dependent regulation of lipid droplet formation and fatty acid uptake.

## MATERIALS AND METHODS

### Mice

The floxed Rar $\alpha$  (Rar $\alpha^{fl/fl}$ ) mice (on a C57BL/6 background) were generously gifted by Dr. Yasmine Balkaid (National Institutes of Health/National Institute of Allergy and Infectious Diseases) and have been previously described by Dr. Chambon and colleagues.<sup>[10]</sup> Albumin cre (Alb-Cre) mice were purchased from the Jackson Laboratory. Rar $\alpha^{fl/fl}$  mice were crossed with Alb-cre mice to generate germline hepatocyte-specific Rar $\alpha^{-/-}$  (gL-Rar $\alpha^{-/-}$ ) and control littermates (Rar $\alpha^{fl/fl}$  mice). AAV8-TBG-Null or AAV8-TBG-Cre was intravenously injected to 8-week-old male Rar $\alpha^{fl/fl}$  mice to generate control mice (Rar $\alpha^{fl/fl}$ ) or adult-onset hepatocyte-specific Rar $\alpha^{-/-}$  (L-Rar $\alpha^{-/-}$ ) mice, respectively. Some of the mice were also gavaged with either vehicle (0.5% carboxymethyl cellulose) or AtRA (15 mg/kg/day).<sup>[7]</sup> All mice were housed in a temperature and humidity-controlled room with a 12-h light/12-h dark cycle under pathogen-free conditions. Mice are fasted for 5–6 h during the light cycle before euthanasia. All animal experiments were approved by the Institutional

Animal Care and Use Committee at Northeast Ohio Medical University.

### Diets

The HFCF diet contained 40% fat, 0.2% cholesterol (AIN-76A Western diet from TestDiet), and 4.2% fructose (in drinking water). Eight-week-old male mice were used and fed an HFCF diet for 16 or 20 weeks. The high-fat diet (HFD) containing 60% kcal from fat was purchased from Research Diets (Cat. #D12492). Eight-week-old mice were used and fed an HFD for 20 weeks.

### Adeno-associated viruses

Adeno-associated virus 8 (AAV8)-TBG-null (control) and AAV8-TBG-Cre were produced and titrated by Vector BioLabs. Each mouse was intravenously injected with  $3 \times 10^{11}$  genome copies of AAVs.

### Primary hepatocyte isolation and culture

Mouse primary hepatocytes were isolated as described.<sup>[11]</sup> Mice were anesthetized by intraperitoneal injection of Xylazine/Ketamine. The portal vein was cannulated with a 23-gauge plastic cannula. Mouse livers were perfused with Hank's Balanced Salt Solution (HBSS; 14170112; Thermo Fisher Scientific). Subsequently, livers were perfused with HBSS with calcium and magnesium (14,025,092; Thermo Fisher Scientific) containing 0.8 mg/ml collagenase from *Clostridium histolyticum* type IV (Sigma). Primary hepatocytes were released and collected in a 50-ml centrifuge tube. After centrifugation at 50g for 3 min and washing with Dulbecco's modified Eagle's medium (DMEM), cells were cultured in DMEM plus 10% fetal bovine serum (FBS) in plates or 6-well dishes pre-coated with 0.1% gelatin. Primary hepatocytes were cultured in DMEM containing vehicle or lipid mixture (100  $\mu$ m palmitate, 100  $\mu$ m oleic acid, 100  $\mu$ m linoleic acid, and 1  $\mu$ g/ml cholesterol). After 24 or 48 h, messenger RNA (mRNA) levels and intracellular lipid levels were determined.

### Real-time polymerase chain reaction

Total RNA was isolated using Trizol Reagent (Invitrogen), and mRNA levels were quantified by quantitative real-time PCR (PCR) using PowerUP SYBR Green Master Mix (Thermo Fisher) on a 7500 Real-Time PCR machine (Applied Biosystems). Results were calculated

using cycle threshold values and normalized to 36B4 mRNA level.

### Analysis of intracellular and hepatic lipids

About 100-mg livers were homogenized in methanol, and lipids in the livers or hepatocytes were extracted in chloroform/methanol (2:1 vol/vol) as described previously.<sup>[12]</sup> Hepatic and intracellular triglyceride and total cholesterol levels were quantified using Infinity reagents from Thermo Fisher Scientific. Free cholesterol and nonesterified free fatty acids (NEFAs) were determined using a kit from Wako Chemicals USA.

### Analysis of plasma aspartate aminotransferase, alanine aminotransferase, and lipids and hepatic hydroxyproline

Plasma triglycerides, cholesterol, glucose, aspartate aminotransferase (AST) and alanine aminotransferase (ALT) levels were determined using Infinity reagents from Thermo Scientific. NEFAs were determined using a kit from Wako Chemicals USA. About 40–50 mg of the liver was homogenized in distilled water and hydroxyproline levels in the liver were quantified using a kit from Cell BioLabs (Cat. #STA675).

### Oil Red O, hematoxylin and eosin, or picrosirius red staining

Liver tissues were fixed in 10% formalin and then embedded in optimal cutting temperature or paraffin. Liver sections were stained with Oil Red O (ORO), hematoxylin and eosin (H&E), or picrosirius red. Images were acquired using an Olympus microscope.

### Body composition analysis and energy expenditure

Mouse body fat mass was measured by EchoMRI-700 (Echo Medical Systems). Oxygen consumption, carbon dioxide production, heat production, and physical activity were determined in a Comprehensive Lab Animal Monitoring System using Columbus Instruments hardware and Oxymax software (Columbus Instruments) as detailed previously.<sup>[13]</sup> In brief, mice underwent an acclimation period, and a 24-h measurement of energy expenditure was determined using an eight-chamber system. Each run included two genotypes and two treatments with two mice per group.

### Fatty acid oxidation

Primary hepatocytes were isolated, and then cultured in DMEM containing 10% FBS in 12-well dishes in the presence of vehicle or AtRA (2  $\mu$ m). After 48 h, the media were removed and washed with 1 $\times$  phosphate-buffered saline. The cells were then cultured in DMEM containing 0.5% fatty acid-free BSA, 0.5  $\mu$ Ci [<sup>3</sup>H]palmitate, and 500  $\mu$ m cold palmitate. Radioactivity was measured and fatty acid oxidation (FAO) was determined as described previously.<sup>[14,15]</sup>

### Fatty acid uptake

Primary hepatocytes were isolated and plated at  $5 \times 10^4$  cells per well in 96-well plates. Cells were incubated in DMEM plus 10% FBS in the presence of vehicle or AtRA (4  $\mu$ m) overnight. Before the assay, hepatocytes were fasted 2 h by changing to a serum-free media. Fatty acid uptake was measured using a QBT fatty acid uptake assay kit (Molecular Devices) by reading the plate at 485 nm excitation/535 nm emission. The end-point fatty acid uptake after 1 h was determined as described.<sup>[16]</sup>

### Hepatic lipogenesis

Mice were fasted for 2 h and then injected intraperitoneally with <sup>2</sup>H<sub>2</sub>O (20–30  $\mu$ l/g). After 4 h, liver and plasma were snap-frozen. The newly synthesized triglycerides were measured by gas chromatography–mass spectrometry as described.<sup>[17]</sup>

### Intestinal fat absorption and hepatic very-low density lipoprotein secretion

To determine intestinal fat absorption, mice were fasted for 6 h, and then intravenously injected with 100  $\mu$ l Tyloxapol (500 mg/kg). Mice were then gavaged with olive oil (15  $\mu$ l/g body weight) and plasma triglyceride (TG) levels were determined at defined time points as described previously.<sup>[18,19]</sup> For the VLDL secretion assay, mice were fasted for 6 h and then intravenously injected with 100–200  $\mu$ l of Tyloxapol (500 mg/kg). Blood was collected at indicated time points and plasma TG levels were determined.

### Statistical analysis

All data were expressed as mean  $\pm$  SEM. Statistical significance was analyzed using an unpaired Student *t* test or analysis of variance (ANOVA; for more than two groups) by using GraphPad Prism (GraphPad

Software). Differences were considered statistically significant at  $p < 0.05$ .

## RESULTS

### RAR $\alpha$ is required to protect against intracellular lipid accumulation in hepatocytes

To determine the role of hepatocyte RAR $\alpha$  in lipid metabolism, we isolated primary hepatocytes from *Rar $\alpha$ <sup>fl/fl</sup>* mice and mice with germline deficiency of *Rar $\alpha$*  in hepatocytes (*gL-Rar $\alpha$ <sup>-/-</sup>*), and treated them with a lipid cocktail of free fatty acids and cholesterol

because they are known to be elevated in NAFLD. Loss of hepatocyte *Rar $\alpha$*  significantly increased cellular levels of TG (Figure 1A), NEFAs (Figure 1B), total cholesterol (TC), and free cholesterol (FC) (Figure 1C). Consistent with these findings, quantitative real-time PCR data show that some genes were induced by *Rar $\alpha$*  deficiency, including genes involved in lipogenesis (peroxisome proliferator-activated receptor  $\gamma$ 1 (*Ppar $\gamma$ 1*), *Ppar $\gamma$ 2*, acetyl-CoA carboxylase 1 (*Acc1*), *Acc2*) or lipid droplet formation (cell death–inducing DNA fragmentation factor-like effector A [*Cidea*], *Cidec*, perilipin 4 [*Plin4*]), or inflammation (tumor necrotic factor  $\alpha$  (*Tnfa*)) (Figure 1D). *Rar $\alpha$*  deficiency inhibited the expression of peroxisome proliferator-activated receptor  $\beta/\delta$  (*Ppar $\beta/\delta$* ), but had no impact on the expression

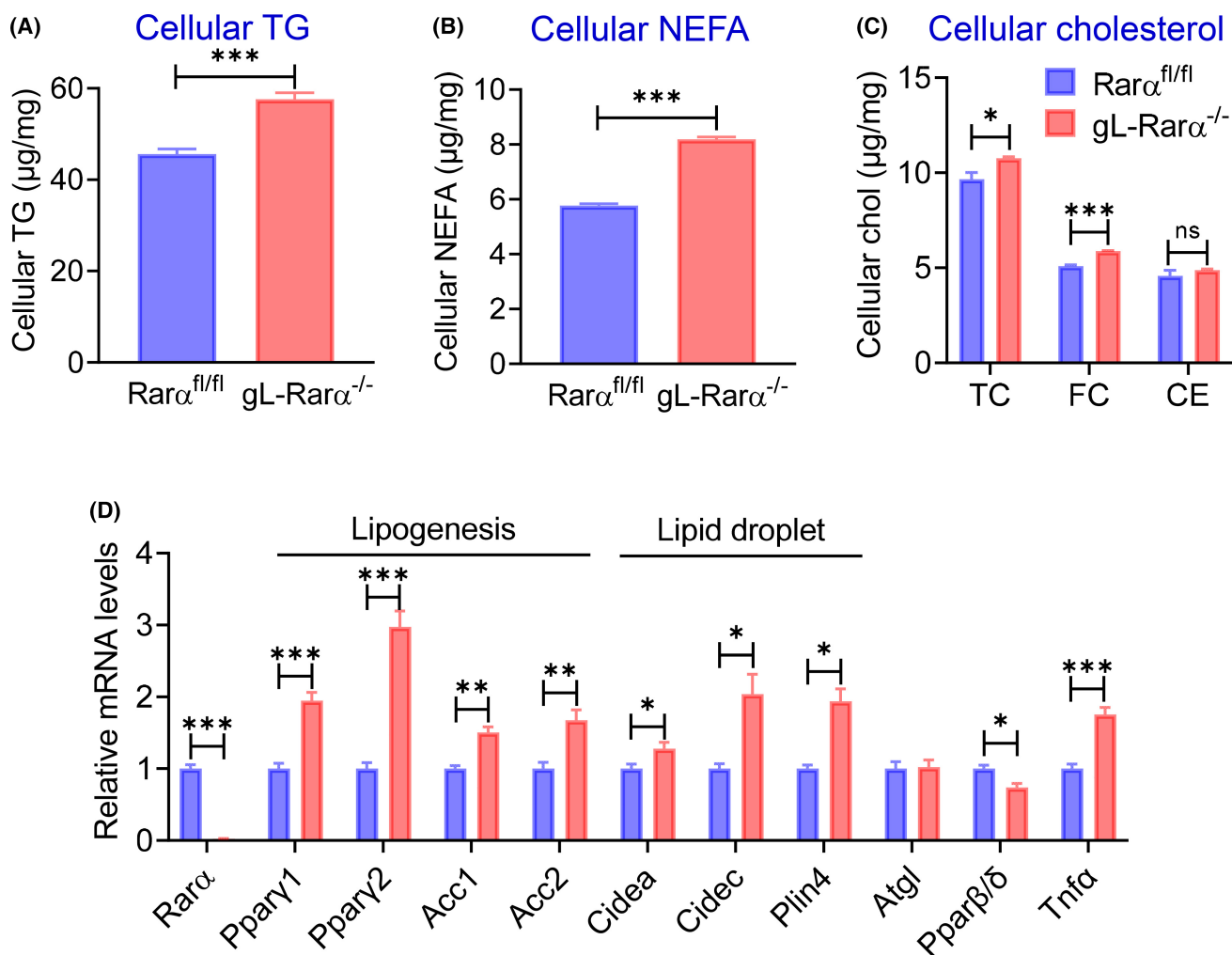


**FIGURE 1** Retinoid acid receptor alpha (RAR $\alpha$ ) is required to protect against intracellular lipid accumulation in hepatocytes. Primary hepatocytes were isolated from *Rar $\alpha$ <sup>fl/fl</sup>* mice and mice with germline deficiency in *Rar $\alpha$*  (*gL-Rar $\alpha$ <sup>-/-</sup>*) and cultured in the presence of lipids (100  $\mu$ M oleic acid, linoleic acid, palmitic acid, and 1  $\mu$ g/ml cholesterol) for 48 h (intracellular lipids) and 24 h (messenger RNA [mRNA]). Intracellular levels of triglycerides (TG) (A), nonesterified fatty acids (NEFAs) (B), total cholesterol (TC), free cholesterol (FC), and cholesterol esters (CE) (C) were measured. (D) mRNA levels were determined. All values are expressed as mean  $\pm$  SEM; \* $p < 0.05$ , \*\* $p < 0.01$ , \*\*\* $p < 0.001$ . *Acc1*, acetyl-CoA carboxylase 1; *Atgl*, adipose triglyceride lipase; Chol, cholesterol; ns, not significant; *Cidea*, cell death–inducing DNA fragmentation factor-like effector A; *Plin4*, perilipin 4; PPAR $\gamma$ , peroxisome proliferator-activated receptor gamma; *Tnfa*, tumor necrosis factor alpha.

of genes involved in lipolysis, such as adipose triglyceride lipase (*Atgl*) (Figure 1D).

## Germline loss of hepatocyte RAR $\alpha$ induces hepatosteatosis in chow-fed aged mice

To determine whether hepatocyte RAR $\alpha$  affected the development of NAFLD on a chow diet, we studied 1-year-old male *Rara*<sup>fl/fl</sup> mice versus *gL-Rara*<sup>-/-</sup> mice. Compared with *Rara*<sup>fl/fl</sup> mice, *gL-Rara*<sup>-/-</sup> mice had significantly higher body weight, body fat content (%), and plasma NEFA levels, whereas the ratio of the liver to body weight and plasma levels of glucose, TG, or cholesterol were unchanged (Figure S1A–G).

Surprisingly, *gL-Rara*<sup>-/-</sup> mice had higher plasma AST and ALT levels (Figure 2A), indicative of liver injury in these mice (Figure 2A). *gL-Rara*<sup>-/-</sup> mice also had higher levels of TG (Figure 2B) and NEFA (Figure 2C) in the liver, whereas hepatic TC or FC was unchanged despite a subtle increase in cholesterol ester (CE) levels (Figure 2D). Histological staining with Oil Red O or H&E showed increased hepatosteatosis in *gL-Rara*<sup>-/-</sup> mice (Figure 2E). Consistent with the increased hepatic lipid accumulation, hepatic

mRNA levels involved in lipogenesis (sterol regulatory element binding protein 1c [*Srebp1c*], *Acc1*, *Acc2*, ATP-citrate lyase (*Acly*)) and lipid droplet formation (*Cidea*, *Plin4*) were significantly increased (Figure 2F). Hepatic *Cd36* and diacylglycerol acyltransferase 1 (*Dgat1*) also tended to increase (Figure 2F). Thus, germline loss of hepatocyte RAR $\alpha$  is sufficient to induce hepatosteatosis on a chow diet.

## Germline loss of hepatocyte RAR $\alpha$ induces hepatosteatosis in HFD-fed mice

Next, we fed 8-week-old male *Rara*<sup>fl/fl</sup> mice and *gL-Rara*<sup>-/-</sup> mice a HFD (60% kcal from fat) or a chow diet for 20 weeks. In HFD-fed mice we observed a modest increase in the plasma NEFA levels in *gL-Rara*<sup>-/-</sup> mice, but there was no change in body weight, body fat content, the ratio of liver to body weight, hepatic cholesterol (TC, FC, and CE), or plasma levels of glucose, TG, or TC between *Rara*<sup>fl/fl</sup> mice and *gL-Rara*<sup>-/-</sup> mice (Figure S2A–H). However, there was a >50% increase in plasma AST and ALT levels (Figure 3A,B), hepatic TG (Figure 3C), and hepatic NEFA (Figure 3D) levels in HFD-fed *gL-Rara*<sup>-/-</sup> mice compared with HFD-fed *Rara*<sup>fl/fl</sup> mice with no changes observed in the

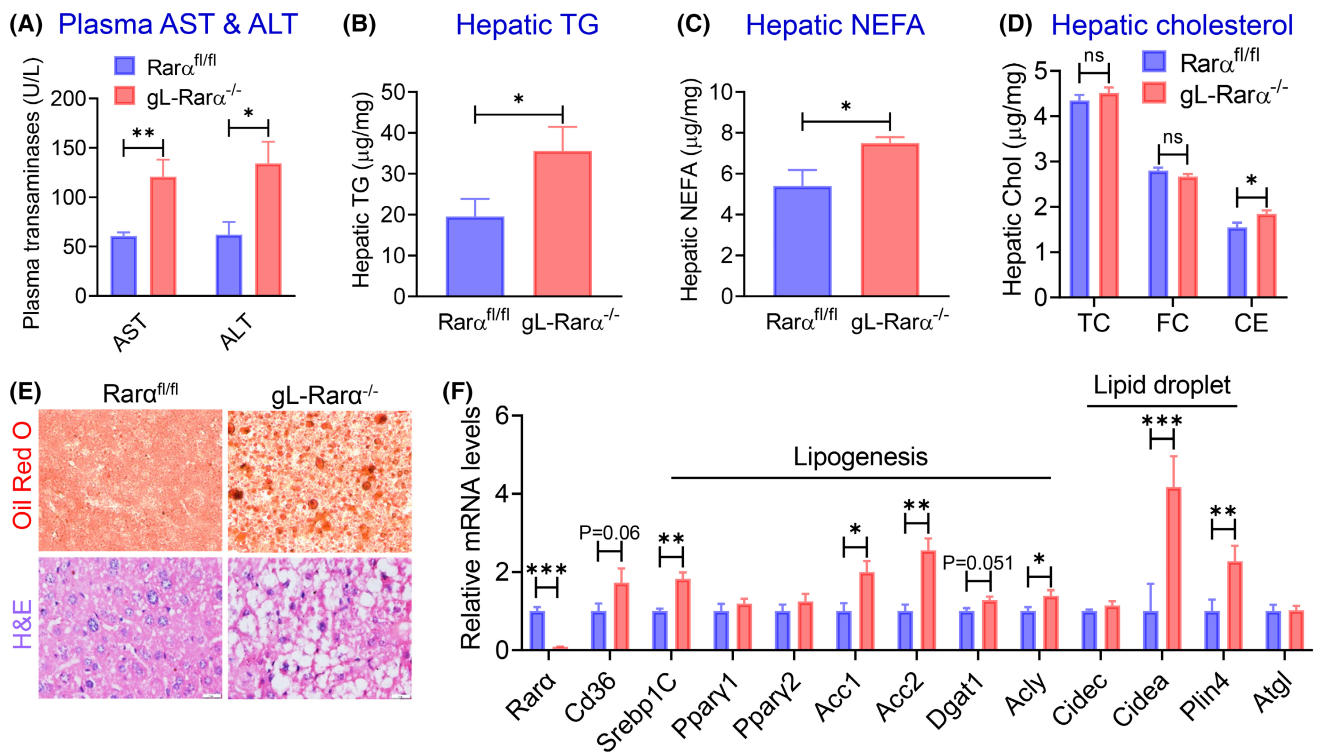


**FIGURE 2** Germline loss of hepatocyte RAR $\alpha$  induces hepatosteatosis in chow-fed aged mice. One-year-old male *Rara*<sup>fl/fl</sup> mice and *gL-Rara*<sup>-/-</sup> male mice were fed a chow diet (n = 7–8). Plasma aspartate aminotransferase (AST) and alanine aminotransferase (ALT) levels (A) as well as hepatic levels of TG (B), NEFA (C), TC, FC, and CE were determined. (E) Representative liver images of Oil Red O staining (upper panels) and hematoxylin and eosin (H&E) staining (lower panels) (scale bars = 20 μm). (F) Hepatic mRNA levels were quantified. All values are expressed as mean ± SEM; \*p < 0.05, \*\*p < 0.01, \*\*\*p < 0.001. ns, not significant. *Acly*, ATP citrate lyase; *Cd36*, cluster of differentiation 36; *Dgat1*, diacylglycerol o-acyltransferase 1; *Srebp1C*, sterol regulatory element-binding protein 1C.

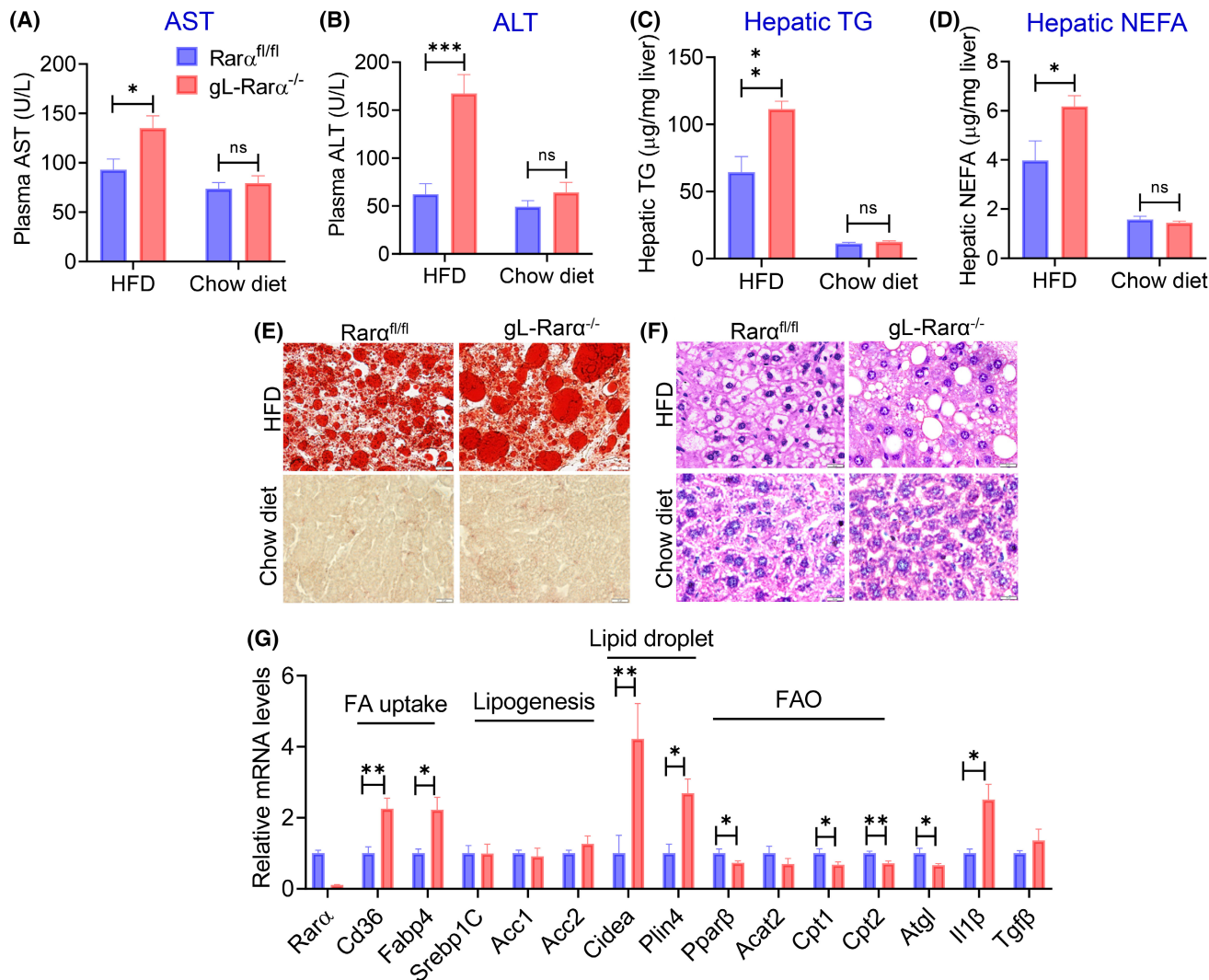


**FIGURE 3** Germline loss of hepatocyte RAR $\alpha$  induces hepatosteatosis in high-fat diet-fed mice. Eight-week-old male *Rar $\alpha$ <sup>fl/fl</sup>* and *gL-Rar $\alpha$ <sup>-/-</sup>* mice were fed a high-fat diet (HFD) (n = 7) or a chow diet (n = 8) for 20 weeks. Plasma AST (A) and ALT (B) levels, and hepatic TG (C) and NEFA (D) levels were determined. (E,F) Representative liver images of Oil Red O staining (E) and H&E staining (F) (scale bars = 20  $\mu$ m). (G) Hepatic mRNA levels of HFD-fed mice were measured. All values are expressed as mean  $\pm$  SEM; \* $p$  < 0.05, \*\* $p$  < 0.01, \*\*\* $p$  < 0.001. Cpt1, carnitine palmitoyltransferase 1; FA, fatty acid; FAO, fatty acid oxidation; *Fabp4*, fatty acid binding protein 4; *Il1 $\beta$* , interleukin 1 $\beta$ ; *Tgfb $\beta$* , tumor growth factor $\beta$ .

age-matched chow-fed mice (Figure 3A–D). The increase in hepatic TG accumulation was also confirmed by ORO staining and H&E staining in HFD-fed mice with no significant changes in ORO or H&E staining in chow-fed mice (Figure 3E,F).

In the liver, genes involved in fatty acid uptake (*Cd36*, fatty acid binding protein 4 [*Fabp4*]), lipid droplet formation (*Cidea*, *Plin4*), and inflammation (interleukin-1 $\beta$ ) were significantly induced, whereas genes involved in FAO (*Ppar $\beta$* , carnitine palmitoyl transferase 1 [*Cpt1*], *Cpt2*) or lipolysis (*Atgl*) were significantly reduced (Figure 3G). Interestingly, genes involved in lipogenesis (*Srebp1c*, *Acc1*, *Acc2*) or fibrogenesis (transforming growth factor  $\beta$ ) were unchanged (Figure 3G). Thus, the data in Figure 3 indicate that germline loss of hepatocyte RAR $\alpha$  aggravates HFD-induced hepatosteatosis.

### AtRA protects from HFCF diet-induced obesity in a hepatocyte RAR $\alpha$ -dependent manner

To determine whether hepatocyte RAR $\alpha$  played a role in AtRA-mediated regulation of lipid homeostasis, we intravenously injected AAV8-TBG-null or AAV8-TBG-iCRE to *Rar $\alpha$ <sup>fl/fl</sup>* mice to generate adult-onset hepatocyte-specific *Rar $\alpha$*  knockout (*L-Rar $\alpha$ <sup>-/-</sup>*) mice and their control mice. These mice were then fed a HFCF diet with a daily gavage with either vehicle or AtRA (15 mg/kg) for 16 weeks. Interestingly, AtRA reduced body weight (Figure 4A) and body fat content (Figure 4B) in *Rar $\alpha$ <sup>fl/fl</sup>* mice but not in the *L-Rar $\alpha$ <sup>-/-</sup>* mice. Consistent with these observations, AtRA increased oxygen consumption (Figure 4C), CO<sub>2</sub> production (Figure 4D), and energy expenditure (Figure 4E) during the day and dark time in *Rar $\alpha$ <sup>fl/fl</sup>* mice but not in

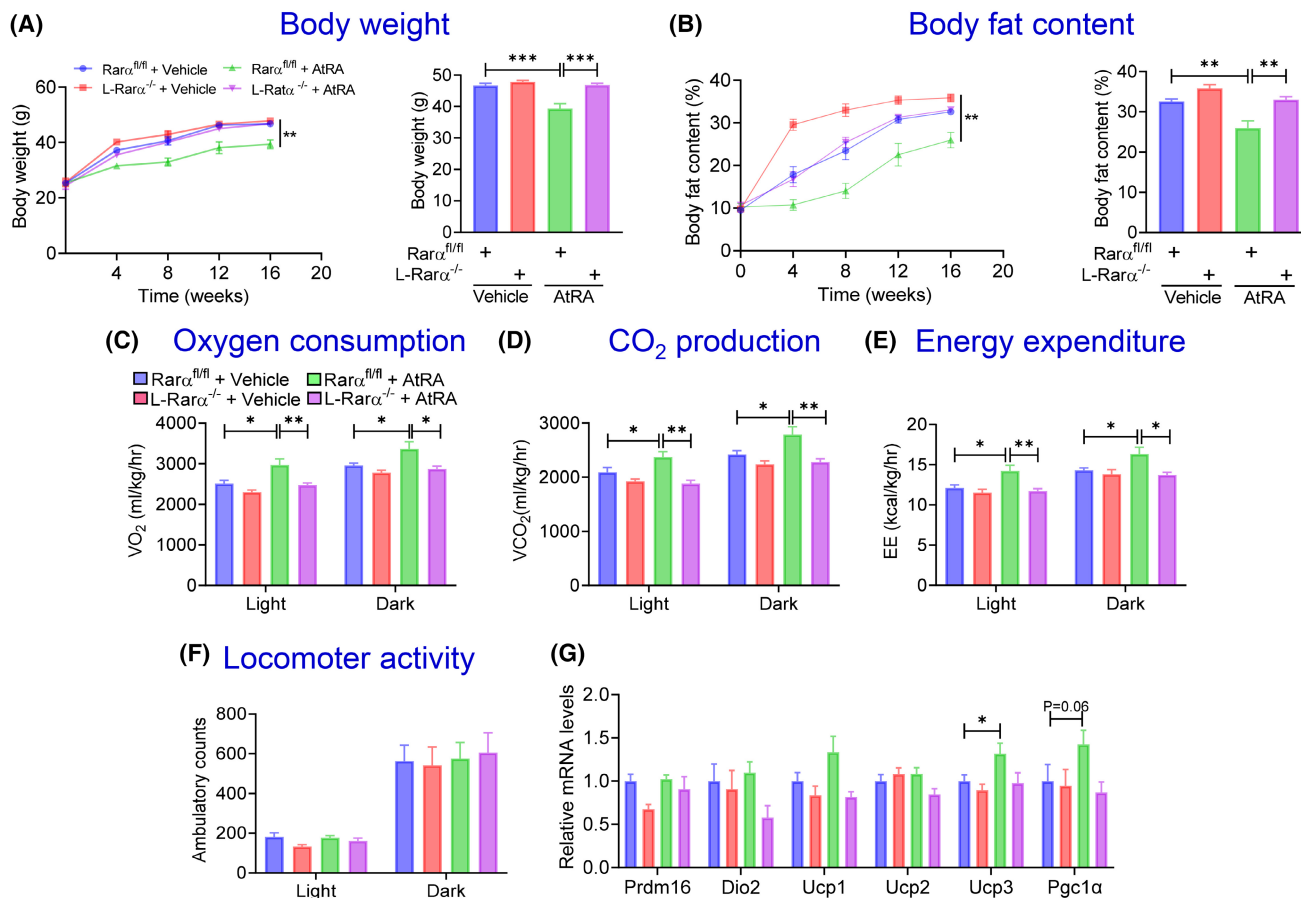


**FIGURE 4** All-trans retinoic acid (AtRA) protects from high fat/cholesterol/fructose (HFHF) diet-induced obesity in a hepatocyte RAR $\alpha$ -dependent manner. *Rar $\alpha^{fl/fl}$*  mice were intravenously injected with adeno-associated virus 8 (AAV8)-TBG-null or AAV8-TBG-iCRE and then gavaged with vehicle or AtRA (15 mg/kg) for 16 weeks ( $n = 8$  per group). These mice were also fed a HFHF diet. Body weight over the 16 weeks (A, left panel) or for the final week (A, right panel) was measured. Body fat content over the 16 weeks (B, left panel) or the for the final week (B, right panel) was determined. Oxygen consumption (C), CO<sub>2</sub> production (D), energy expenditure (E), and ambulatory locomotor activity (F) during the 24-h light or dark time were analyzed. mRNA levels in brown adipose tissue were determined (G). All values are expressed as mean  $\pm$  SEM; \* $p < 0.05$ , \*\* $p < 0.01$ , \*\*\* $p < 0.001$ . *Dio2*, iodothyroine deiodinase 2; *Pgc1 $\alpha$* , peroxisome proliferator-activated receptor gamma coactivator 1- $\alpha$ ; *Prdm16*, PR domain containing 16; *UCP1*, uncoupling protein 1.

the *L-Rar $\alpha^{-/-}$*  mice. There was no change in locomotor activity (Figure 4F). In brown adipose tissue, there was a modest increase in uncoupled protein 3 (*Ucp3*) and a tendency in induction of peroxisome proliferator-activated receptor gamma coactivator 1 $\alpha$  (*Pgc1 $\alpha$* ) in the *L-Rar $\alpha^{-/-}$*  mice (Figure 4G). These results indicate that retinoic acid prevents HFHF diet-induced obesity via hepatocyte RAR $\alpha$ -dependent induction of energy expenditure.

### AtRA protects from HFHF diet-induced hepatosteatosis in a RAR $\alpha$ -dependent manner

Previous studies have shown that AtRA treatment ameliorates diet-induced hepatosteatosis in mice.<sup>[8]</sup> However, it is unclear whether hepatocyte RAR $\alpha$  plays a role in this process. The data in Figure 5 show that AtRA modestly reduced plasma ALT and AST levels (Figure 5A) as well as the ratio of the liver to body weight (Figure 5B), and decreased hepatic TG levels by 67%

(Figure 5C) in *Rar $\alpha^{fl/fl}$*  mice. However, these reductions were largely abolished in *L-Rar $\alpha^{-/-}$*  mice (Figure 5A–C). The data from ORO staining (Figure 5D) or H&E staining (Figure 5E) further confirmed these findings. Interestingly, AtRA treatment had not much effect on hepatic NEFA, cholesterol, or hydroxyproline levels in *Rar $\alpha^{fl/fl}$*  mice but reduced hepatic NEFA, TC, and FC levels in *L-Rar $\alpha^{-/-}$*  mice (Figure S3A–D), suggesting that AtRA may regulate hepatic NEFA, TC, or FC levels in the absence of hepatocyte RAR $\alpha$ . These results indicate that hepatocyte RAR $\alpha$  is important for AtRA to attenuate diet-induced hepatosteatosis.

### AtRA reduces hepatosteatosis by inhibiting hepatocyte fatty acid uptake and lipid droplet formation via hepatocyte RAR $\alpha$

To understand how AtRA attenuates HFHF diet-induced hepatosteatosis via hepatocyte RAR $\alpha$ , we

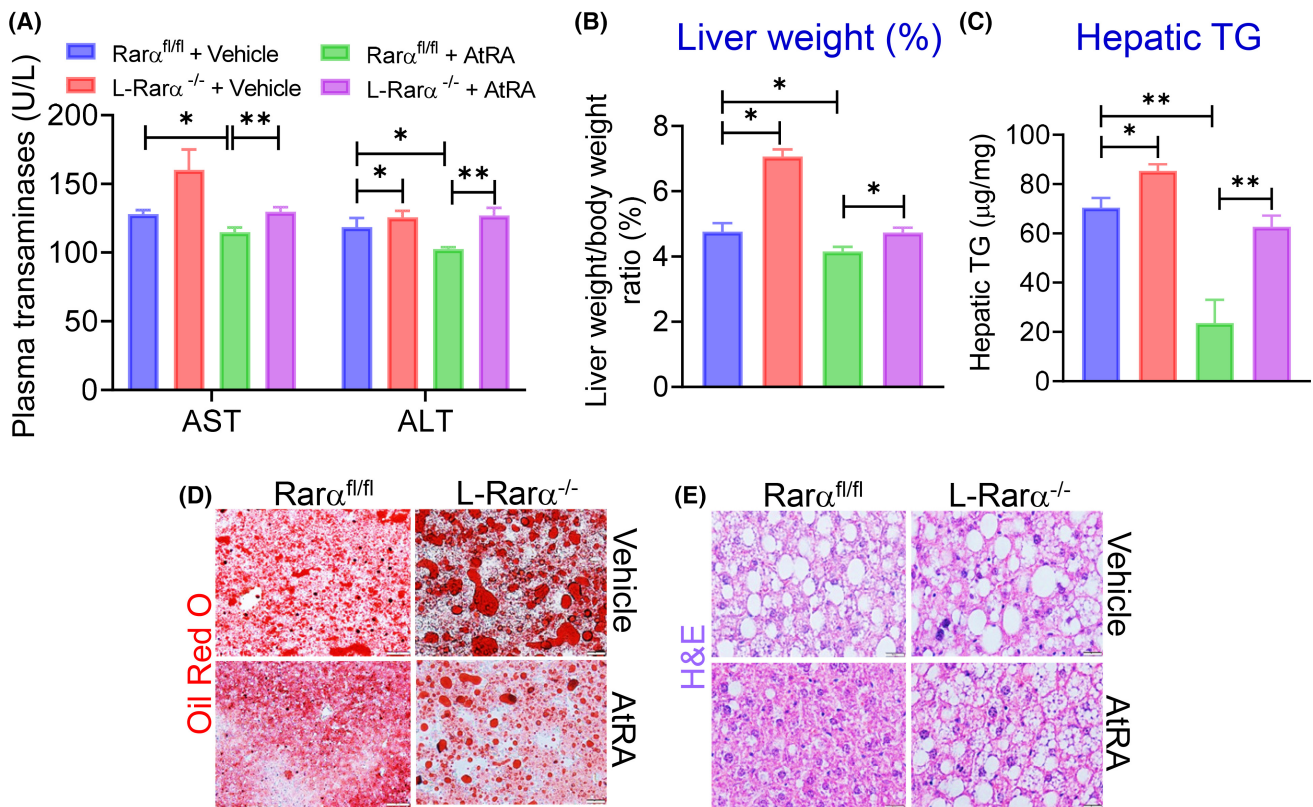


**FIGURE 5** AtRA protects from HFCF diet–induced hepatosteatosis in a RAR $\alpha$ -dependent manner. *Rar $\alpha^{fl/fl}$*  mice were intravenously injected with AAV8-TBG-null or AAV8-TBG-iCRE and then gavaged with vehicle or AtRA (15 mg/kg) for 16 weeks ( $n = 8$  per group). These mice were also fed a HFCF diet. (A) Plasma AST and ALT levels were analyzed. (B) The liver weight–to–body weight ratio (percentage) was measured. (C) Hepatic TG levels were quantified. (D,E) Representative liver images of Oil Red O staining (D) or hematoxylin and eosin (H&E) staining (E) are presented (scale bars = 20  $\mu$ m). All values are expressed as mean  $\pm$  SEM; \* $p < 0.05$ , \*\* $p < 0.01$ .

measured hepatic gene expression and performed some functional assays. AtRA treatment inhibited the expression of genes involved in lipid droplet formation (*Cidea*, *Cidec*, *Plin2*, *Plin3*, *Plin4*, *Plin5*) or fatty acid uptake (*Cd36*, *Fabp4*) in the *Rar $\alpha^{fl/fl}$*  mice, and these reductions were largely abolished in *L-Rar $\alpha^{-/-}$*  mice (Figure 6A,B). Although AtRA treatment reduced some of the genes involved in lipogenesis (*Srebp1c*, *Pparg1*, *Pparg2*, *Scd1*, *Scd2*), other lipogenic genes (*Acc1*, *Acc2*, *Fasn*) were unchanged (Figure 6D). Importantly, AtRA did not regulate hepatic TG synthesis although loss of hepatocyte RAR $\alpha$  significantly induced hepatic TG synthesis (Figure 6D). AtRA reduced hepatic apolipoprotein b and microsomal triglyceride transfer protein expression, but did not have much impact on hepatic genes involved in FAO (*Cpt1*, *Cpt2*, *Ppar $\alpha$* ) except for a significant induction of *Cpt1c* (Figure 4A,B). Further studies showed that loss of hepatocyte RAR $\alpha$  did not affect VLDL secretion or intestinal fat absorption (Figure 4C,D).

We then determined the role of AtRA in fatty acid uptake and FAO by hepatocytes. AtRA treatment reduced fatty acid uptake in *Rar $\alpha^{fl/fl}$*  mice but not in *L-Rar $\alpha^{-/-}$*  mice (Figure 6E). In contrast, AtRA induced FAO in both *Rar $\alpha^{fl/fl}$*  mice and *L-Rar $\alpha^{-/-}$*  mice (Figure 6F).

Taken together, the data in Figures 5 and 6 indicate that AtRA prevents diet-induced hepatosteatosis through hepatocyte RAR $\alpha$ -dependent inhibition of fatty acid uptake and lipid droplet formation.

### AtRA reverses HFCF diet–induced obesity and hepatosteatosis dependent on hepatocyte RAR $\alpha$

To investigate whether AtRA could reverse HFCF diet–induced hepatosteatosis, we fed *Rar $\alpha^{fl/fl}$*  mice and *gL-Rar $\alpha^{-/-}$*  mice an HFCF diet for 20 weeks. During the last 10 weeks, these mice were also gavaged with either vehicle or AtRA. Treatment with AtRA significantly reduced body weight (Figure 7A,B), body fat content (Figure 7C), and hepatic TG levels (Figure 7D) in the *Rar $\alpha^{fl/fl}$*  mice, and these reductions were largely abolished in the *L-Rar $\alpha^{-/-}$*  mice (Figure 7A–D). The changes in hepatic TG levels were also corroborated by hepatic ORO staining (Figure 7E) and H&E staining (Figure 7F). Thus, the data in Figure 7 show that hepatocyte RAR $\alpha$  is essential for AtRA to reverse diet-induced obesity and hepatosteatosis.



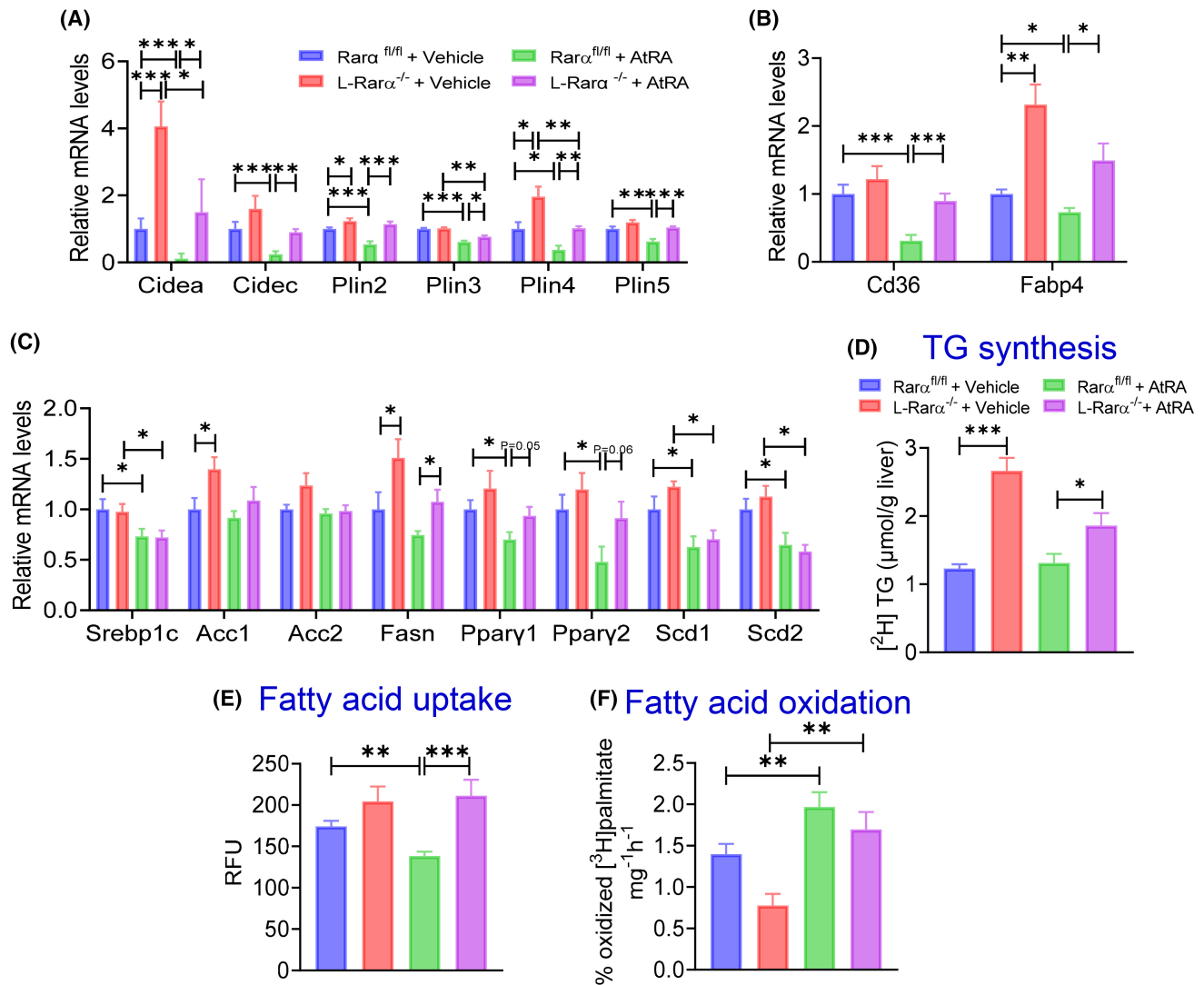


**FIGURE 6** AtRA reduces hepatosteatosis by inhibiting hepatocyte fatty acid uptake and lipid droplet formation. *Rara*<sup>fl/fl</sup> mice were intravenously injected with AAV8-TBG-null or AAV8-TBG-iCRE and then gavaged with vehicle or AtRA (15 mg/kg) for 16 weeks (n = 8 per group). These mice were also fed a HFCF diet. Hepatic mRNA levels of genes involved in lipid droplet formation (A), fatty acid uptake (B), and lipogenesis (C) were determined. (D) Hepatic newly synthesized TG levels were analyzed. (E) Fatty acid uptake was determined in primary hepatocytes treated with either vehicle or AtRA (4 μM) (n = 10 per group). (F) FAO was performed in isolated primary hepatocytes treated with either vehicle or AtRA (2 μM), with each well seeded with the same amounts of cells. All values are expressed as mean ± SEM; \**p* < 0.05, \*\**p* < 0.01, \*\*\**p* < 0.001. RFU, relative fluorescence unit.

## DISCUSSION

Clinical studies have shown that retinoic acid signaling is impaired in NAFLD.<sup>[4–6]</sup> Treatment of mice<sup>[7]</sup> or rabbits<sup>[8]</sup> with AtRA attenuates diet-induced hepatosteatosis, suggesting that impaired retinoic acid signaling may promote or aggravate the development of NAFLD. Indeed, our current studies show that loss of RARα in hepatocytes is sufficient to cause hepatosteatosis in aged mice or HFD-fed mice. In line with our studies, expression of dominant negative RARα in the liver is also shown to promote liver steatosis.<sup>[20]</sup>

Aging is known to promote hepatic steatosis, and the progression of NAFLD via cellular senescence and impaired mitochondrial activity.<sup>[21,22]</sup> Retinoic

acid signaling is known to enhance mitochondrial activity.<sup>[23]</sup> However, the role of RARα in senescence is not well understood. Our studies show that loss of hepatic RARα aggravates steatosis in 1-year-old mice but not in age-matched wild-type mice. It will be interesting to investigate whether hepatocyte senescence plays a role in hepatic steatosis induced by RARα deficiency.

So far, the exact mechanism by which AtRA inhibits liver steatosis remains to be fully understood. A previous study show that AtRA may prevent hepatosteatosis via inhibition of PPARγ signaling.<sup>[7]</sup> AtRA is known to function via activation of RARα, RARβ or RARγ, which are expressed in many tissues and cell types. In the current study, we demonstrate that

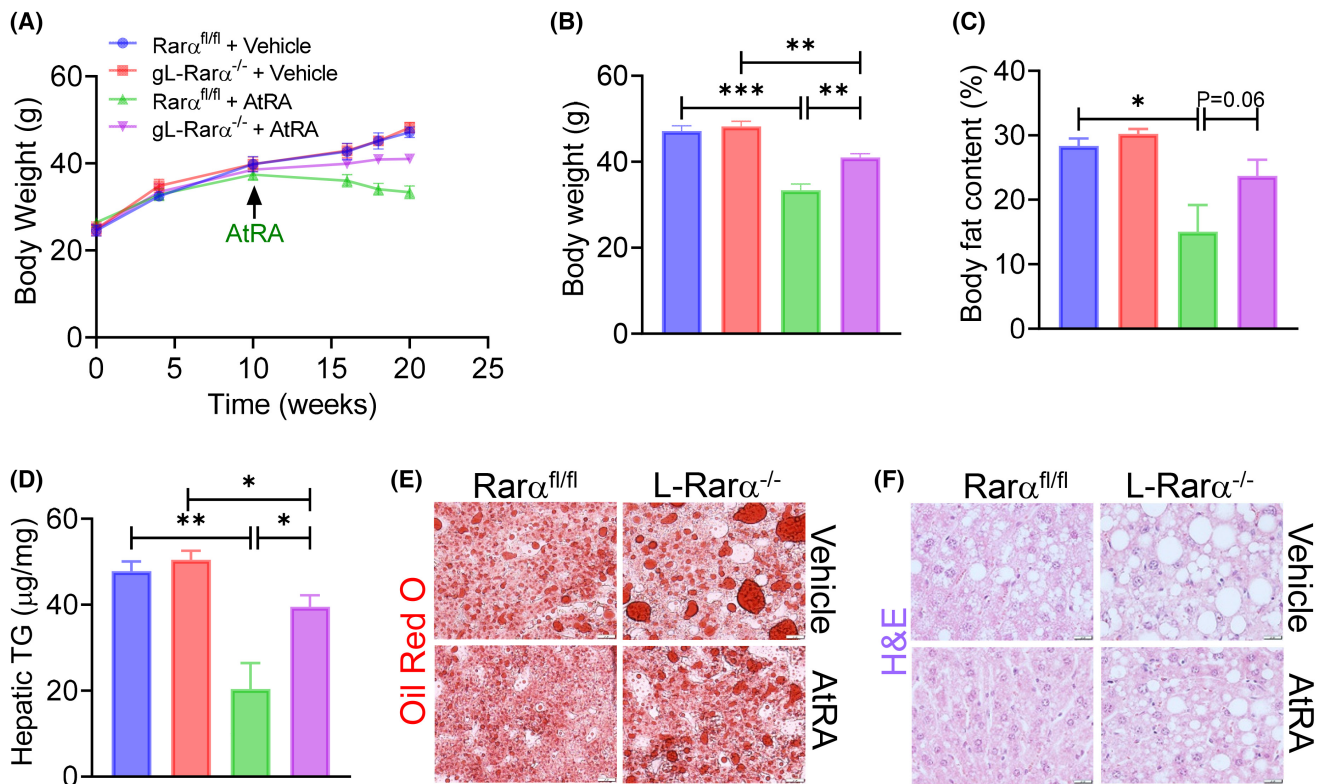


**FIGURE 7** AtRA reverses HFCF diet–induced obesity and hepatosteatosis dependent on hepatocyte RAR $\alpha$ . Eight-week-old male  $Rar\alpha^{fl/fl}$  mice and  $gL-Rar\alpha^{-/-}$  mice were fed an HFCF diet for a total of 20 weeks. After they were fed an HFCF diet for 10 weeks, they were also gavaged with vehicle or AtRA (15 mg/kg, once a day) for another 10 weeks. (A) Body weight over the 20 weeks was measured. (B,C) At the conclusion of the study, body weight (B) and body fat content (C) were also measured. (D) Hepatic TG levels were determined. (E,F) Representative liver images of Oil Red O staining (E) and H&E staining (F) are shown (scale bars = 20  $\mu\text{m}$ ). All values are expressed as mean  $\pm$  SEM; \* $p$ <0.05, \*\* $p$ <0.01, \*\*\* $p$ <0.001.

AtRA attenuates diet-induced liver steatosis via activation of hepatocyte RAR $\alpha$  and subsequent inhibition of fatty acid uptake by hepatocytes and lipid droplet formation. AtRA promotes FAO in both  $Rar\alpha^{fl/fl}$  mice and  $L-Rar\alpha^{-/-}$  mice, suggesting that AtRA-regulated FAO does not play a role in RAR $\alpha$ -mediated reduction of hepatosteatosis. Also, we show that AtRA does not regulate hepatic TG synthesis or hepatic expression of genes involved in lipolysis or VLDL secretion. Collectively, our data indicate that AtRA ameliorates diet-induced hepatosteatosis via hepatocyte RAR $\alpha$ -mediated inhibition of hepatic fatty acid uptake and lipid droplet formation.

In addition to attenuating diet-induced hepatosteatosis, AtRA treatment also prevents diet-induced obesity in a hepatocyte RAR $\alpha$ -dependent manner. A previous study shows that activation of RAR $\beta$  induces hepatic fibroblast growth factor 21 to stimulate FAO and promote whole body energy metabolism.<sup>[24]</sup> Nonetheless, we still do not fully understand how activation of hepatic RAR $\alpha$  is responsible for AtRA to induce energy expenditure and inhibit diet-induced obesity.

Because activation of hepatic RAR $\alpha$  prevents and reverses hepatosteatosis, and retinoic acid signaling is

impaired in NAFLD, targeting hepatic RAR $\alpha$  or retinoic acid signaling may be a promising strategy for treatment of hepatosteatosis. Whether and how retinoic acid signaling regulates steatohepatitis remains to be explored.

#### AUTHOR CONTRIBUTIONS

*Study concept and design, data interpretation, and manuscript preparation:* Fathima N. Cassim Bawa and Yanqiao Zhang. *Experiments:* Fathima N. Cassim Bawa, Yanyong Xu, Raja Gopaju, Amy Shiyab, Shuwei Hu, Shaoru Chen, Yingdong Zhu, and Kavita Jadhav. *Data analysis:* Noel-Marie Plonski. *Gas chromatography–mass spectrometry studies:* Takhar Kasumov.

#### FUNDING INFORMATION

Supported by the National Institutes of Health (R01DK102619 and R01DK118941).

#### CONFLICT OF INTEREST

Nothing to report.

#### ORCID

Yanqiao Zhang  <https://orcid.org/0000-0002-1886-7775>

## REFERENCES

1. Loomba R, Friedman SL, Shulman GI. Mechanisms and disease consequences of nonalcoholic fatty liver disease. *Cell*. 2021;184:2537–64.
2. Friedman SL, Neuschwander-Tetri BA, Rinella M, Sanyal AJ. Mechanisms of NAFLD development and therapeutic strategies. *Nat Med*. 2018;24:908–22.
3. Pan X, Zhang Y. Hepatocyte nuclear factor 4alpha in the pathogenesis of non-alcoholic fatty liver disease. *Chin Med J (Engl)*. 2022 Feb 21. <https://doi.org/10.1097/CM9.0000000000002092>. [Epub ahead of print]
4. Saeed A, Dullaart RPF, Schreuder T, Blokzijl H, Faber K. Disturbed vitamin A metabolism in non-alcoholic fatty liver disease (NAFLD). *Nutrients*. 2017;10:29.
5. Zhong G, Kirkwood J, Won KJ, Tjota N, Jeong H, Isoherranen N. Characterization of vitamin a metabolome in human livers with and without nonalcoholic fatty liver disease. *J Pharmacol Exp Ther*. 2019;370:92–103.
6. Chaves GV, Pereira SE, Saboya CJ, Spitz D, Rodrigues CS, Ramalho A. Association between liver vitamin A reserves and severity of nonalcoholic fatty liver disease in the class III obese following bariatric surgery. *Obes Surg*. 2014;24:219–24.
7. Kim SC, Kim CK, Axe D, Cook A, Lee M, Li T, et al. All-trans-retinoic acid ameliorates hepatic steatosis in mice by a novel transcriptional cascade. *Hepatology*. 2014;59:1750–60.
8. Zarei L, Farhad N, Abbasi A. All-trans retinoic acid (atRA) effectively improves liver steatosis in a rabbit model of high fat induced liver steatosis. *Arch Physiol Biochem*. 2020;23:1–6.
9. Tsuchiya H, Ikeda Y, Ebata Y, Kojima C, Katsuma R, Tsuruyama T, et al. Retinoids ameliorate insulin resistance in a leptin-dependent manner in mice. *Hepatology*. 2012;56:1319–30.
10. Chapellier B, Mark M, Messaddeq N, Calléja C, Warot X, Brocard J, et al. Physiological and retinoid-induced proliferations of epidermis basal keratinocytes are differently controlled. *EMBO J*. 2002;21:3402–13.
11. Edwards M, Houseman L, Phillips IR, Shephard EA. Isolation of mouse hepatocytes. *Methods Mol Biol*. 2013;987:283–93.
12. Bligh EG, Dyer WJ. A rapid method of total lipid extraction and purification. *Can J Biochem Physiol*. 1959;37:911–7.
13. Zhang Y, Ge X, Heemstra LA, Chen WD, Xu J, Smith JL, et al. Loss of FXR protects against diet-induced obesity and accelerates liver carcinogenesis in ob/ob mice. *Mol Endocrinol*. 2012;26:272–80.
14. Rune A, Osler ME, Fritz T, Zierath JR. Regulation of skeletal muscle sucrose, non-fermenting 1/AMP-activated protein kinase-related kinase (SNARK) by metabolic stress and diabetes. *Diabetologia*. 2009;52:2182–9.
15. Li Y, Zalzal M, Jadhav K, Xu Y, Kasumov T, Yin L, et al. Carboxylesterase 2 prevents liver steatosis by modulating lipolysis, endoplasmic reticulum stress, and lipogenesis and is regulated by hepatocyte nuclear factor 4 alpha in mice. *Hepatology*. 2016;63:1860–74.
16. Liao J, Sportsman R, Harris J, Stahl A. Real-time quantification of fatty acid uptake using a novel fluorescence assay. *J Lipid Res*. 2005;46:597–602.
17. Xu J, Li Y, Chen WD, Xu Y, Yin L, Ge X, et al. Hepatic carboxylesterase 1 is essential for both normal and farnesoid X receptor-controlled lipid homeostasis. *Hepatology*. 2014;59:1761–71.
18. Khalifeh-Soltani A, McKleroy W, Sakuma S, Cheung YY, Tharp K, Qiu Y, et al. Mfge8 promotes obesity by mediating the uptake of dietary fats and serum fatty acids. *Nat Med*. 2014;20:175–83.
19. Xu Y, Li Y, Jadhav K, Pan X, Zhu Y, Hu S, et al. Hepatocyte ATF3 protects against atherosclerosis by regulating HDL and bile acid metabolism. *Nat Metab*. 2021;3:59–74.
20. Yanagitani A, Yamada S, Yasui S, Shimomura T, Murai R, Murawaki Y, et al. Retinoic acid receptor alpha dominant negative form causes steatohepatitis and liver tumors in transgenic mice. *Hepatology*. 2004;40:366–75.
21. Ogrodnik M, Miwa S, Tchkonja T, Tiniakos D, Wilson CL, Lahat A, et al. Cellular senescence drives age-dependent hepatic steatosis. *Nat Commun*. 2017;8:15691.
22. Aravinthan A, Scarpini C, Tachtatzis P, Verma S, Penrhyn-Lowe S, Harvey R, et al. Hepatocyte senescence predicts progression in non-alcohol-related fatty liver disease. *J Hepatol*. 2013;58:549–56.
23. Tripathy S, Chapman JD, Han CY, Hogarth CA, Arnold SLM, Onken J, et al. All-trans-retinoic acid enhances mitochondrial function in models of human liver. *Mol Pharmacol*. 2016;89:560–74.
24. Li Y, Wong K, Walsh K, Gao B, Zang M. Retinoic acid receptor beta stimulates hepatic induction of fibroblast growth factor 21 to promote fatty acid oxidation and control whole-body energy homeostasis in mice. *J Biol Chem*. 2013;288:10490–504.

## SUPPORTING INFORMATION

Additional supporting information can be found online in the Supporting Information section at the end of this article.

**How to cite this article:** Cassim Bawa FN, Xu Y, Gopaju R, Plonski N-M, Shiyab A, Hu S, et al. Hepatic retinoic acid receptor alpha mediates all-trans retinoic acid's effect on diet-induced hepatosteatosis. *Hepatol Commun*. 2022;6:2665–2675. <https://doi.org/10.1002/hep4.2049>